Factorization at fixed $Q^2(1-x)$

Paul Hoyer,[a] **Matti Järvinen**[b] **and Samu Kurki**[a]

[a]*Department of Physics and Helsinki Institute of Physics,*
POB 64, FIN-00014 University of Helsinki,
Helsinki, Finland
[b]*High Energy Physics Center, University of Southern Denmark,*
Campusvej 55, DK-5230 Odense M, Denmark
E-mail: `paul.hoyer@helsinki.fi`, `mjarvine@imada.sdu.dk`,
`samu.kurki@helsinki.fi`

ABSTRACT: We consider QCD factorization between hard and soft subprocesses in inclusive reactions where the momentum fraction x of one parton approaches unity as the hard scale $Q^2 \to \infty$, such that $Q^2(1-x)$ is fixed. In this "BB limit" the entire (multi-parton) Fock state containing the high x parton is coherent with the hard subprocess. The soft contribution is given by a forward multiparton matrix element. The BB limit corresponds to a fixed (large or small) missing mass and is thus closely connected to exclusive production. We analyze the Drell-Yan process $h + N \to \gamma^* + X$ in detail, explaining why the virtual photon is longitudinally polarized for $h = \pi$ and transversely polarized for $h = p$. The BB limit may be relevant also for other phenomena observed at high x, such as the large single spin asymmetries of $pp \to \Lambda^\uparrow X$ and in $pp^\uparrow \to \pi X$.

KEYWORDS: Deep Inelastic Scattering, QCD.

Contents

1. The BB limit

Data on hard inclusive processes has been successfully analyzed assuming QCD factorization between a hard subprocess and universal soft matrix elements (parton distributions). Formally one considers the leading contributions in the Bj limit where a hard scale $Q^2 \to \infty$ while the momentum fractions x_i carried by the active partons (one in each hadron) are held fixed. The higher twist corrections are power suppressed in the hard scale but generically increase as $x_i \to 1$. Thus the effective expansion parameter is $1/[Q^2(1 - x_i)]$ (see [1] for a recent phenomenological analysis of $eN \to eX$ (DIS)).

Data at high x has features which differ qualitatively from the leading twist contribution. A striking example is the polarization of the virtual photon in $\pi N \to \mu^+ \mu^- X$ which changes from transverse to longitudinal when the photon carries a momentum fraction $x_F \gtrsim 0.6$ of the pion beam [2]. This requires that at least one of the annihilating quarks in the subprocess $q\bar{q} \to \gamma^*(Q^2)$ goes off-shell by an amount commensurate with the photon virtuality Q^2. As pointed out by Berger and Brodsky [3] the longitudinally polarized photon is coherent with both valence quarks in the pion. Hence the dominant contribution is of higher twist even though the subprocess is hard. An analogous change of J/ψ polarization at high x_F was observed in $\pi N \to J/\psi + X$ [4]. The inapplicability of the twist expansion in QCD at high x was discussed in [5].

In this paper we consider QCD factorization in a limit where $x \to 1$ as $Q^2 \to \infty$. Here x can denote either the momentum fraction x_i of a fast quark i or equivalently the x_F of a final state particle. The Drell-Yan data suggests that the helicity of the pion is transferred

to the virtual photon at high x, implying that the photon is coherent with an entire Fock state of the pion. The life-time of a Fock state is inversely proportional to ΔE, the energy difference between the pion and the Fock state. At high pion momentum p,

$$2p\Delta E \simeq m_\pi^2 - \sum_i \frac{p_{i\perp}^2 + m_i^2}{x_i} \tag{1.1}$$

The $x \simeq 1$ quark which annihilates into the virtual photon contributes only little to the energy difference (1.1). The life-time of the Fock state is determined by the stopped partons with $x_i \propto 1 - x$. If $1 - x \sim \Lambda_{\rm QCD}^2/Q^2$ we get $2p\Delta E \sim Q^2$ (we take $p_{i\perp} \sim \Lambda_{\rm QCD}$, a generic soft QCD scale). Such Fock states have life-times similar to that of the virtual photon, ensuring their coherence with the hard process. This motivates us to consider the

$$\text{BB limit}: \quad Q^2 \to \infty \quad \text{at fixed} \quad Q^2(1-x) \tag{1.2}$$

which recognizes [6] the early observations of Berger and Brodsky [3].

The understanding of QCD factorization in the BB limit is facilitated by an analogy with ordinary DIS ($ep \to eX$). In the rest frame of the target DIS may be viewed [7] as proceeding through a splitting of the virtual photon into a quark pair, $\gamma^*(Q^2) \to q\bar{q}$. The quark carries nearly all of the photon energy ν and forms the current jet, whereas the antiquark carries a finite momentum in the target rest frame, even as $\nu = Q^2/2m_p x_B \to \infty$. The $q\bar{q}$ Fock state of the photon is analogous to the pion Fock state we just discussed: A fast quark with momentum fraction $x_q \simeq 1$ and an antiquark with $x_{\bar{q}} \sim \Lambda_{\rm QCD}^2/Q^2$. The fact that the momentum $x_{\bar{q}}\nu$ of the antiquark remains finite in the Bj limit allows the alternative (standard) interpretation of the antiquark as a quark constituent of the proton. The DIS cross section can then be equivalently ascribed to the scattering of the $q\bar{q}$ Fock state on the target or to the probability of finding a quark in the target wave function. The latter interpretation corresponds to the parton distributions obtained in QCD factorization.

In the following we shall analyze factorization of the Drell-Yan process in the BB limit, interpreting stopped partons in Fock states of the beam as (anti-)parton constituents of the target. We do not consider rescattering effects, i.e. , gauge links between the quark fields [8].

2. Kinematics of $\pi^+ N \to \gamma^* + X$ at fixed $(1 - x_F)Q^2$

Our notation for the $\pi^+ N \to \gamma^* + X$ kinematics is indicated in the Feynman diagram of figure 1. The pion, nucleon and photon momenta are in Light-Front (LF) notation ($k = (k^+, k^-, \boldsymbol{k}_\perp)$ with $k^\pm = k^0 \pm k^3$)

$$\begin{aligned} \text{Pion}: \quad & k = (0, k^-, \boldsymbol{0}_\perp) \\ \text{Nucleon}: \quad & p = (p^+, m_N^2/p^+, \boldsymbol{0}_\perp) \\ \text{Photon}: \quad & q = (Q^2/q^-, q^-, \boldsymbol{q}_\perp) \end{aligned} \tag{2.1}$$

We neglect the mass of the pion as we take its momentum $k^- \to \infty$. We work in the target rest frame, $p^+ = p^- = m_N$, thus $s = (k + p)^2 \simeq m_N k^- \to \infty$. In the BB limit
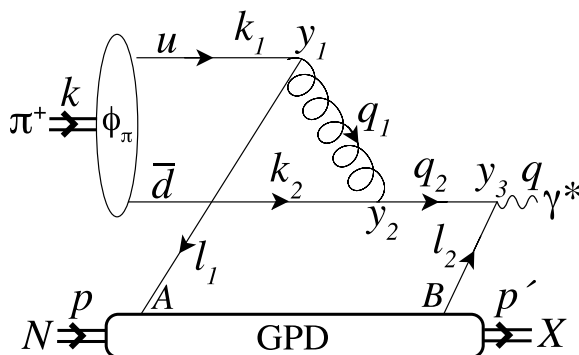
Figure 1: Feynman diagram contributing to the $T_d(\pi N \to \gamma^* X)$ amplitude. The arrows indicate momentum directions; the y_i are space-time positions of the vertices and A, B denote color indices. The pion contributes via its $u\bar{d}$ distribution amplitude ϕ_π and the GPD denotes a transition $(N \to X)$ Generalized Parton Distribution.

$x_F \equiv q^-/k^- \to 1$ at fixed $\boldsymbol{q}_\perp$, keeping also

$$x_B \equiv \frac{q^+}{p^+} = \frac{Q^2}{s} \quad \text{fixed} \tag{2.2}$$

$$k^- - q^- \equiv x_M p^- = \frac{Q^2(1 - x_F)}{q^+} \quad \text{fixed}$$

Since the four-momentum transfer $k - q$ to the target system is fixed the invariant mass M_X of the hadronic state X is finite in the BB limit,

$$M_X^2 = (k + p - q)^2 \simeq (1 - x_B)[s(1 - x_F) + m_N^2] - \boldsymbol{q}_\perp^2 \tag{2.3}$$

and may be small or large depending on the value of $s(1 - x_F) = Q^2(1 - x_F)/x_B$. For $X = N$ we have the exclusive Drell-Yan process $\pi N \to \gamma^* N$ [10] as well as the time-reversed version of $\gamma^* N \to \pi^+ N$ (Deeply Exclusive Meson Production) which are well-known to be described by Generalized Parton Distributions [11] as indicated in figure 1. Factorization [12] applies equally to the transition GPD's $(X \neq N)$ [13, 14] since $M_X \ll Q$. In section 3 we merely sketch the derivation of the factorized amplitude.

In section 4 we consider the factorization of the inclusive Drell-Yan cross section $\sigma(\pi^+ N \to \mu\mu X)$ through a completeness sum over the states X. As in the standard leading twist limit of the Drell-Yan process, this includes integrating over the (small) transverse momentum $\boldsymbol{q}_\perp$ of the virtual photon, which arises from the intrinsic momentum of the partons in the GPD. High transverse momenta are suppressed at fixed M_X since the GPD is expected to fall off $\propto 1/\boldsymbol{q}_\perp^4$, similarly to nucleon transition form factors. The integration over $\boldsymbol{q}_\perp$ can be done at fixed M_X by varying $(k-q)^-$ without affecting the hard subprocess at leading order.

We anticipate that the pion will contribute through its distribution amplitude $\phi_\pi(z)$ and parametrize the momenta of its valence quarks as

$$k_1 = \left(0, zk^-, \boldsymbol{k}_\perp\right)$$
$$k_2 = \left(0, (1 - z)k^-, -\boldsymbol{k}_\perp\right) \tag{2.4}$$
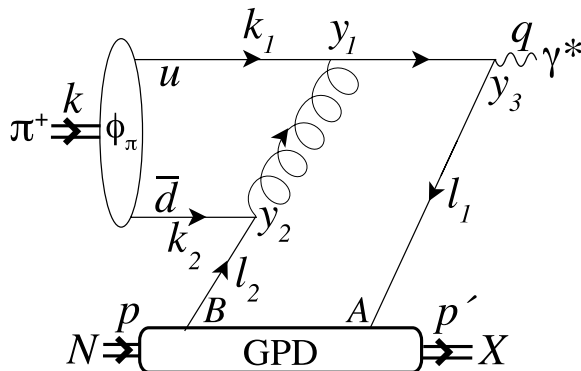
Figure 2: Feynman diagram contributing to $T_u(\pi^+ N \to \gamma^* X)$. Notations as in figure 1.

We take the transverse momenta to be limited, $\boldsymbol{k}_\perp^2 \ll Q^2$. Thus we neglect the perturbative tail of the wave function which arises from gluon exchange and gives rise to the logarithmic Q^2 evolution of the distribution amplitude [9]. k_1^+ and k_2^+ vanish in the high energy limit and do not contribute at leading order.

In the BB limit (1.2) one of the quarks in the pion (the u-quark in figure 1) transfers nearly all its momentum to the other quark, such that the photon carries nearly all of the pion momentum. The stopped u-quark is left with a finite momentum in the target rest frame and should be connected to the target wave function as discussed above for DIS. Consequently, as $k^- \to \infty$,

$$x = l_1^+/p^+ \quad \text{fixed}$$
$$x_B + x = l_2^+/p^+ \quad \text{fixed} \tag{2.5}$$

A large longitudinal momentum is transferred through the gluon (q_1) and quark (q_2) propagators whose virtualities are of $\mathcal{O}\left(Q^2\right)$,

$$\left.\begin{array}{l} q_1^2 \simeq -zk^- l_1^+ \\ q_2^2 \simeq -k^- l_1^+ \end{array}\right\} \propto Q^2 = x_B s \tag{2.6}$$

This implies that the hard interactions occur at nearly the same LF times (y_1^+, y_2^+, $y_3^+ = \mathcal{O}\left(1/k^-\right)$) and vanishing transverse separations ($y_{1\perp}$, $y_{2\perp}$, $y_{3\perp} = \mathcal{O}\left(1/Q\right)$).

Since q_1^2 and q_2^2 are independent of l_i^- and $l_{i\perp}$ the soft target matrix element will be integrated over these components (with the kinematic constraint $l_1 - l_2 = k - q$). In evaluating the hard, perturbative subprocess it suffices to take

$$l_1 = (xp^+, 0^-, \mathbf{0}_\perp)$$
$$l_2 = ((x + x_B)p^+, 0^-, \mathbf{0}_\perp) \tag{2.7}$$

and analogously only the minus components in (2.4) contribute. Thus both quarks effectively reverse their direction of motion along the z-axis.

3. Drell-Yan amplitude in the BB limit

The general expression for the scattering amplitude is

$$iT(\pi^+ N \to \gamma_\lambda^* X)(2\pi)^4 \delta^4(k + p - q - p')$$
$$= \langle \gamma_\lambda^* X | \mathrm{T} \left\{ \exp\left[-i \int dt H_I(t) \right] \right\} | \pi N \rangle \tag{3.1}$$

The expression for a diagram such as in figure 1 is obtained by expanding the hard vertices of the interaction Hamiltonian H_I, connecting them by perturbative propagators and retaining the leading contribution in the BB limit (2.2). Equivalently, we may simply note that due to the large momenta of $\mathcal{O}(k^-)$ flowing from $y_1 \to y_2 \to y_3$ the corresponding LF time differences $y_2^+ - y_1^+$ and $y_3^+ - y_2^+$ are of $\mathcal{O}(1/k^-)$. Similarly, the squared transverse separations vanish as the inverse virtualities (2.6): $|\boldsymbol{y}_{2\perp} - \boldsymbol{y}_{1\perp}|$ and $|\boldsymbol{y}_{3\perp} - \boldsymbol{y}_{2\perp}|$ are of $\mathcal{O}(1/Q)$. The diagram may then be evaluated using standard Feynman rules with the prescription (A.14) (see appendix A) for the pion. The quarks l_1 and l_2 are treated as external particles and their free wave functions are replaced according to

$$\bar{u}(l_1) \to \int \frac{dl_1^+}{2\pi} \frac{dy_1^-}{2} \langle X(p') | \bar{\psi}_u(y_1) \exp\left(-\frac{1}{2} i y_1^- l_1^+ \right)$$
$$u(l_2) \to \psi_d(0) | N(p) \rangle \tag{3.2}$$

Our conventions for the wave functions and operators are explained in detail in appendix A. Adding the diagram where the gluon vertex y_2 in figure 1 is on the l_2 line we find for the amplitude where a photon of helicity $\lambda = 0$ is emitted from the d-quark,

$$T_d(\pi^+ N \to \gamma_L^* X) = e_d \frac{-ieg^2 C_F}{Q\sqrt{2N_c}} \tag{3.3}$$
$$\times \int \frac{dz \, dl_1^+}{z} \frac{\phi_\pi(z)}{2\pi(l_1^+ - i\varepsilon)} \int dy_1^- e^{-iy_1^- l_1^+/2} \langle X(p') | \bar{\psi}_u(y_1) \gamma^+ \gamma_5 \, \psi_d(0) | N(p) \rangle_{y_1^+ = y_{1\perp} = 0}$$

where $\phi_\pi(z)$ is the pion distribution amplitude. The amplitude for transversely polarized photons is suppressed by a factor $1/Q$. We give an intuitive explanation of this in section 5.

The contribution from the diagrams where the photon is emitted from the u-quark as in figure 2 is obtained in a similar way. Defining

$$C(x_B, x) \equiv \int_0^1 dz \, \phi_\pi(z) \left(\frac{e_u}{1-z} \frac{1}{x_B + x + i\varepsilon} + \frac{e_d}{z} \frac{1}{x - i\varepsilon} \right) \tag{3.4}$$

the Drell-Yan amplitude for longitudinal photons is

$$T(\pi^+ N \to \gamma_L^* X) = T_u + T_d = \frac{-ieg^2 C_F}{2\pi Q\sqrt{2N_c}} \int dx C(x_B, x) \tag{3.5}$$
$$\times \int dy_1^- e^{-iy_1^- l_1^+/2} \langle X(p') | \bar{\psi}_u(y_1) \gamma^+ \gamma_5 \, \psi_d(0) | N(p) \rangle_{y_1^+ = y_{1\perp} = 0}$$

where x and x_B are defined in (2.5). For $X = N$ we may verify that the amplitude indeed corresponds to the usual expression for deeply exclusive pion production [12]. For general states X the matrix element is a "transition" GPD [13, 14].

The full amplitude including the muon vertex is

$$T(\pi N \to \mu^+ \mu^- X) = T(\pi N \to \gamma_L^* X) \frac{i}{Q^2} \bar{u}(q_1,s)(-ie)\not{\epsilon}_0(q)v(q_2,-s')$$

$$= T(\pi N \to \gamma_L^* X) \frac{ie\sin\theta}{Q}\delta_{ss'} \tag{3.6}$$

where θ is the polar angle of the muon momentum in the muon pair rest frame and s, s' are the muon helicities.

4. The inclusive Drell-Yan cross section

The inclusive cross section is obtained by summing over all final states X,

$$\sigma(\pi^+ N \to \gamma_L^* X) = \frac{1}{2s}\sum_X \int \frac{dq^- d^2\boldsymbol{q}_\perp}{(2\pi)^3 2q^-} |T(\pi^+ N \to \gamma_L^* X)|^2 (2\pi)^4 \delta^4(k+p-q-p') \tag{4.1}$$

where $\sum_X$ is defined by the completeness relation,

$$\sum_X |X\rangle\langle X| \equiv \sum_{n=0}^\infty \int \prod_{i=1}^n \frac{d^3\boldsymbol{p}_i}{(2\pi)^3 2E_i} |\boldsymbol{p}_1,\ldots,\boldsymbol{p}_n\rangle\langle\boldsymbol{p}_1,\ldots,\boldsymbol{p}_n| = 1 \tag{4.2}$$

and $p' = \sum_i p_i$ is the total momentum of the state X.

The momentum conserving δ-functions in (4.1) constrain p' and thus allow only a subset of the states X in the completeness sum (4.2). The restriction on $\boldsymbol{p}'_\perp$ is avoided by summing over all transverse momenta $\boldsymbol{q}_\perp$ of the virtual photon. As mentioned in section 2, large values of $\boldsymbol{q}_\perp$ do not contribute significantly to the sum due to the suppression provided by the GPD's. On the other hand, p'^+ and p'^- are fixed by a measurement of x_B and x_F. Hence we need to incorporate the corresponding δ-functions in the (hermitian conjugate) matrix element:

$$\langle N(p)|\bar{\psi}_d(0)\gamma^+\gamma_5\,\psi_u(y_2)|X(p')\rangle\, 2(2\pi)^2 \delta(p^+-q^+-p'^+)\delta(k^-+p^--q^--p'^-)$$

$$= \frac{1}{2}\int dy_3^+\, dy_3^-\, \langle N(p)|\bar{\psi}_d(y_3)\gamma^+\gamma_5\,\psi_u(y_2+y_3)|X(p')\rangle \exp\left[iy_3\cdot(k-q)\right] \tag{4.3}$$

where $\boldsymbol{y}_{3\perp} = 0$ and we used translation invariance in the matrix element. The full completeness sum is allowed using the matrix element in (4.3), since states X which do not conserve momentum will not contribute after the y_3-integrations. The inclusive cross section (4.1) will thus be given by the multiparton distribution shown in figure 3,

$$f_{d\bar{u}/p}(x_B,x_M;x,x') = \tag{4.4}$$

$$= \frac{1}{4(4\pi)^3}\int dy_1^-\, dy_2^-\, dy_3^-\, dy_3^+ \exp\left\{\frac{1}{2}i\left[-y_1^- l_1^+ + y_2^- l_1^{+\prime} - y_3^- q^+ + y_3^+ x_M p^-\right]\right\}$$

$$\times \langle N(p)|\bar{\psi}_d(y_3)\gamma^+\gamma_5\,\psi_u(y_2+y_3)\,\bar{\psi}_u(y_1)\gamma^+\gamma_5\,\psi_d(0)|N(p)\rangle_{y_{i\perp}=0;\ y_1^+=y_2^+=0}$$

where $x_B = q^+/p^+$, $x = l_1^+/p^+$, $x' = l_1'^+/p^+$ and the scaled '−' momentum transferred to the inclusive system is denoted $x_M = k^-(1-x_F)/p^-$. The inclusive mass M_X is given by x_M as

$$M_X^2 = m_N^2(1-x_B)(1+x_M) - \boldsymbol{q}_\perp^2 \tag{4.5}$$
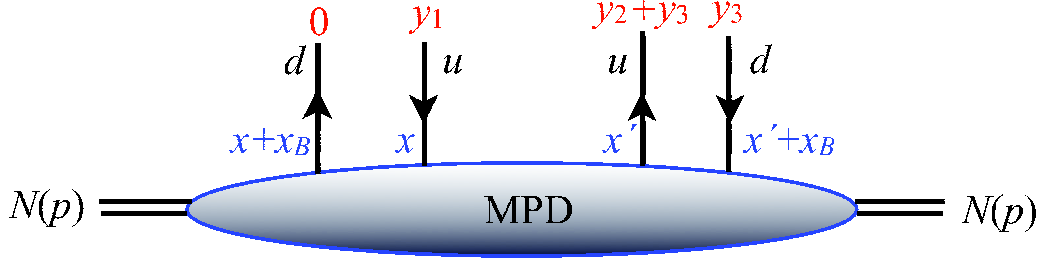
Figure 3: Pictorial representation of the forward multiparton distribution $f_{d\bar{u}/p}(x_B, x_M; x, x')$ given in eq. (4.4).

The kinematic range of x_M in the BB limit is thus

$$\frac{x_B + \boldsymbol{q}_\perp^2/m_N^2}{1 - x_B} \le x_M \le \infty \tag{4.6}$$

The shift by y_3 introduced in (4.3) between the fields in the matrix elements of T and in $T^\dagger$ is conjugate to the momentum transfer $k - q$ between the hard vertex and the target. The MPD (4.4) differs from the higher twist distributions discussed by Jaffe [15] through its dependence on the finite LF time difference y_3^+ between the fields. Also the standard leading twist PDF's are evaluated at $y_3^+ = 0$ since the inclusive system X carries an asymptotically large '$-$' momentum in the Bjorken limit.

In the BB limit the the momentum transfer $x_M p^- = k^-(1 - x_F) = (l_1 - l_2)^- \sim 1/y_3^+$ to the target is kept finite. We may, however, consider the case where this transfer is nevertheless large compared to p^-. Since the quark lines l_1 and l_2 connect to the non-perturbative matrix element their virtualities l_1^2, l_2^2 should remain limited, thus $l_1^+ \sim \Lambda_{\text{QCD}}^2/l_1^-$ and similarly for l_2^+. Given that $l_2^+ - l_1^+ = q^+ = x_B p^+$ is fixed, either l_1^- or $-l_2^-$ may be large, while the other has to be of $\mathcal{O}(p^-)$. If l_1^- is large then $l_1^+ \simeq 0$ and $l_2^+ \simeq q^+$. In this kinematics the u-quark will hadronize independently into a final state jet [3] and the target MPD (4.4) should reduce to a d-quark PDF. We demonstrate this in appendix B.

Using the expression (3.5) of the scattering amplitude in the cross section (4.1) and incorporating the longitudinal δ-function constraints in $T^\dagger$ as in (4.3) the Drell-Yan cross section in the BB limit can be expressed in terms of the double parton distribution (4.4) as

$$\frac{d\sigma(\pi^+ N \to \gamma_L^* X)}{dM_X^2} = \frac{2(eg^2 C_F)^2}{Q^2 s^2(1-x_B)N_c} \int dx dx' C(x_B, x) C^*(x_B, x') f_{d\bar{u}/p}(x_B, x_M; x, x') \tag{4.7}$$

Including the muon pair observables as in (3.6) the differential cross section becomes

$$\frac{d\sigma(\pi^+ N \to \mu\mu X)}{dx_B \, d\Omega_{\mu\mu} \, dM_X^2} = \frac{2\sin^2\theta}{(4\pi)^3 x_B} \frac{d\sigma(\pi^+ N \to \gamma_L^* X)}{dM_X^2} \tag{4.8}$$

5. Photon helicity for pion and proton induced Drell-Yan processes

The fact that the photon is coherent with an entire pion Fock state makes it natural that it also carries the helicity ($\lambda = 0$) of the pion. On the other hand, this argument does not suffice to determine the photon polarization in $pN \to \gamma^* X$, since there is a minimal
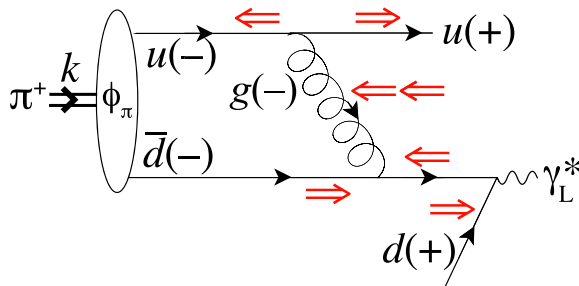
Figure 4: The double red arrows indicate the spin directions of the particles. All momenta are in the $\pm z$-direction as shown in the parentheses. The u-quark propagates into the GPD (not shown) while the d-quark propagates out of it.

helicity flip $|\Delta\lambda| = \frac{1}{2}$ for both transverse and longitudinal photons. The photon was found to be transversely polarized in a calculation of the exclusive $\bar{p}N \to \gamma^*\pi$ process [14]. As we shall see, the same result is obtained for the proton induced inclusive Drell-Yan process in the BB limit.

The helicity systematics follows in a straightforward way from three facts:

(i) The hard interactions conserve quark helicity up to corrections of $\mathcal{O}\left(m_q/Q\right)$;

(ii) Since all transverse momenta $q_\perp$ are limited, orbital contributions $L_z \sim \mathcal{O}\left(q_\perp/Q\right)$;

(iii) Angular momentum $J_z \simeq S_z$ is conserved.

The helicities are then obtained by simple addition. In figure 4 the J_z components are indicated by double arrows in the case $x > 0$ where the u-quark propagates (with positive energy) into the GPD while the d-quark propagates out of it. They follow from helicity conservation for the quark lines, taking into account the direction of longitudinal momentum of the particles (indicated by $\pm$ for motion in the $\pm z$ direction). *E.g.,* the dominant spin component $S_z = -1$ of the gluon may be verified directly by expressing its propagator as a sum over helicities as in (A.3). The quark propagators can analogously be expanded in terms of the spinors (A.10).

The photon polarization in the case of a $J = \frac{1}{2}$ beam particle, such as a nucleon, may be similarly deduced. The analysis is especially simple if we model the nucleon as scalar diquark-quark bound state. Setting $S_z(u) = 0$ in figure 4 gives $S_z(g) = 0$ and consequently $S_z(\gamma^*) = 1$.

We have calculated the relevant diagrams (figure 5) also for three-quark Fock states of a nucleon (see [14] for a corresponding calculation of the exclusive $\bar{p}N \to \gamma^*\pi$ process). Ignoring flavor, the hard subprocess involves nine topologically different diagrams at tree level. See figure 6 for momentum and helicity labels. We parametrize the momenta in analogy to (2.4), (2.7) as

$$k_1 = \left(0^+, z_1 k^-, \boldsymbol{k}_{1\perp}\right)$$
$$k_2 = \left(0^+, z_2 k^-, \boldsymbol{k}_{2\perp}\right)$$
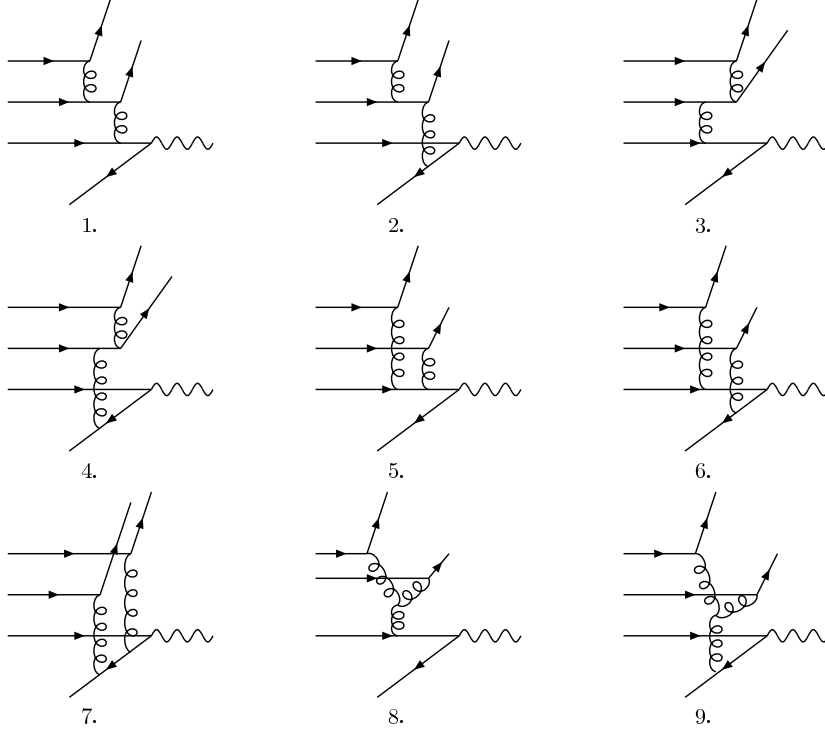
**Figure 5:** Nine topologically different subprocess diagrams in $p\bar{p} \to \gamma^*(x_F) + X$ at large x_F.

$$
\begin{aligned}
k_3 &= \left(0^+, (1 - z_1 - z_2)k^-, -\boldsymbol{k}_{1\perp} - \boldsymbol{k}_{2\perp}\right) \\
\ell_1 &= \left(x_1 p^+, 0^-, \boldsymbol{\ell}_{1\perp}\right) \\
\ell_2 &= \left(x_2 p^+, 0^-, \boldsymbol{\ell}_{2\perp}\right) \\
\ell_3 &= \left(-(x_B + x_1 + x_2)p^+, 0^-, -\boldsymbol{\ell}_{1\perp} - \boldsymbol{\ell}_{2\perp}\right) \\
q &= \left(x_B p^+, x_F k^-, \mathbf{0}_\perp\right)
\end{aligned}
\tag{5.1}
$$

where all transverse momenta ($\sim \Lambda_{\text{QCD}}$) are negligible at leading order in $1/Q$ when evaluating the hard subprocess.

We illustrate the method by calculating the diagram of figure 6 in the BB limit in Feynman gauge. We suppress all color indices and use the light front spinors of (A.10) for the proton valence quarks. Helicity conservation along the quark lines fixes $t_{1,2,3} = s_{1,2,3}$, leaving s_1, s_2, s_3, and λ as parameters. We find that four helicity amplitudes $\mathcal{M}^\lambda_{s_1,s_2,s_3}$ receive contributions at leading order ($\mathcal{M}^\lambda_{s_1,s_2,s_3} \sim 1/Q^3$):

$$
\begin{aligned}
\mathcal{M}^{+1}_{+,-,+} &\simeq \mathcal{M}^{+1}_{-,+,+} \simeq \frac{4\sqrt{2}e_q g^4 \sqrt{x_2(x_1 + x_2 + x_B)z_2(1 - z_1 - z_2)}}{(p^+ k^-)^{3/2}\sqrt{x_1 z_1}(x_1 + x_2)^2(z_1 + z_2)^2} \\
&\simeq \mathcal{M}^{-1}_{-,+,-} \simeq \mathcal{M}^{-1}_{+,-,-}
\end{aligned}
\tag{5.2}
$$

where the lower indices $\pm$ stand for $\pm\frac{1}{2}$ and e_q is the quark charge at the photon vertex. The virtual photon is transverse in the leading amplitudes. This result can also be deduced by using helicity and angular momentum conservation as explained above. The z-components
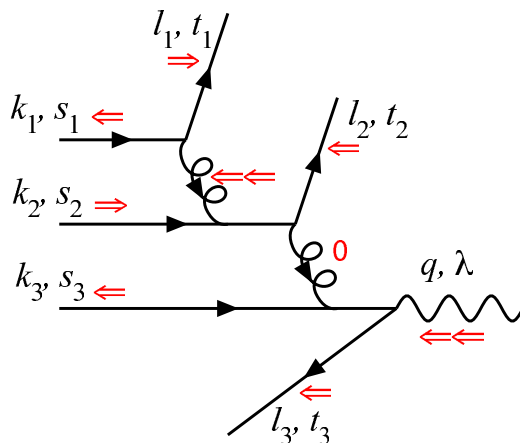
Figure 6: Definitions of momenta (k_i, ℓ_i) and helicities (s_i, t_i) in diagram 1 of figure 5. The red arrows indicate S_z in units of $\frac{1}{2}\hbar$ when $s_1 = -s_2 = s_3 = \frac{1}{2}$ and the photon has helicity $\lambda = 1$. The second gluon carries $S_z = 0$.

of spins are marked with red double arrows in figure 6 for the amplitude $\mathcal{M}^{+1}_{+,-,+}$. Notice that the spin directions match with those of the scalar diquark model above.

We have checked by explicit calculation that the above reasoning applies similarly to all the diagrams of figure 5. We find that the following helicity combinations are leading (fixing $\lambda = +1$):

$$
\begin{array}{rl}
\text{Diagram:} & \text{Helicities:} \\
1,4,8,9 & (s_1, s_2, s_3) = (+,-,+),\ (-,+,+) \\
5 & (s_1, s_2, s_3) = (-,+,+) \\
6 & (s_1, s_2, s_3) = (+,+,-) \\
7 & (s_1, s_2, s_3) = (+,-,+)
\end{array}
\tag{5.3}
$$

Diagrams 2 and 3 do not contribute in Feynman gauge. Contributions with $\lambda = -1$ are obtained from (5.3) by flipping all quark helicities, and amplitudes with $\lambda = 0$ are subleading as expected.

Interestingly, the $(+,+,-)$ amplitude gets a contribution only from diagram 6 of figure 5. This can be understood in terms of helicity conservation since the rules (i)-(iii) imply that for all other diagrams of figure 5 except diagram 6 either a gluon has $|S_z| = 2$ or a quark has $|S_z| = 3/2$. Note that diagram 6 is gauge invariant at leading order in $1/Q$ since both gluons are transverse.

It is also straightforward to check that amplitudes where a pion (proton) projectile produces a transverse (longitudinal) virtual photon are suppressed by orbital factors of $|\boldsymbol{\ell}_{1,2\perp}|/Q$ or $|\boldsymbol{k}_{1,2\perp}|/Q$ as expected from rule (ii) above. In the suppressed amplitudes the projectile wave function is strongly weighted at the endpoints $z = 0, 1$. *E.g.,* the pion distribution amplitude is weighted by $1/z^2$ for $z \to 0$ in the transverse photon amplitude, instead of by $1/z$ as in (3.4). This endangers the convergence of the z-integral and is related to the difficulty of proving factorization for $\gamma_T^* N \to \pi N$ [12].

6. Discussion

The remarkable equality of the inclusive $\gamma^* N \to X$ DIS data at high Q^2 with the exclusive resonance contributions at lower Q^2 [16] points to an intriguing relation between inclusive and exclusive processes. This Bloom-Gilman duality indicates that two mathematical limits simultaneously describe the data: $Q^2 \to \infty$ at fixed x_B and at fixed hadronic (resonance) mass W. The latter limit is equivalent to the BB limit of keeping $Q^2(1 - x_B)$ fixed, some aspects of which we have explored in this paper.

We focussed on the Drell-Yan process $\pi N \to \gamma^* X$ at fixed $Q^2(1 - x_F)$ for the virtual photon. The $x_F \to 1$ limit forces a single quark to carry nearly all the pion momentum. Knowing the "end-point" behaviour of the pion wave function is important in the analysis of its exclusive form factor. The DY data [2] shows that the photon is longitudinally polarized at high x_F, implying that the annihilating quark(s) are far off-shell. This dynamics was studied by Berger and Brodsky [3], who showed that the hard subprocess is different from the standard $q\bar{q} \to \gamma^*$ one and, as in exclusive processes, is coherent with the entire pion Fock state.

The theoretical and experimental evidence of the dominance of a hard subprocess which is suppressed (i.e. , of higher twist) in the usual limit ($Q^2 \to \infty$ at fixed x_F) raised the question whether one can define another limit where this subprocess would be a leading contribution and could be factorized from the soft dynamics. As we discussed in section 1, the requirement of coherence naturally selects the BB limit of fixed $Q^2(1 - x_F)$. Since the mass of the inclusive system X is fixed in this limit the existing factorization proofs for deeply exclusive meson production $\gamma^* N \to \pi N$ [12] apply. The derivation is valid for any fixed mass state X in $\pi N \to \gamma^* X$, which builds the inclusive Drell-Yan process. The elastic process $\pi N \to \gamma^* N$ was already considered in [10]. For $X \neq N$ the soft dynamics involves "Transition Generalized Parton Distributions", which have also been studied previously [13, 14].

We found that $\pi N \to \gamma^* X$ differs essentially from $pN \to \gamma^* X$ in the BB limit since the photon is longitudinally polarized in πN and transversally in pN. Hence the transition from the Bj to the BB limit can be directly observed in πN through the change of photon polarization with increasing x_F. In pN there is (as expected) no evidence for a change of polarization from transverse to longitudinal, and the two limits may coexist in a range of x_F as suggested by duality [16]. This may be connected to the observation that the azimuthal distribution of the muon pair in $pN \to \mu^+\mu^- X$ is consistent with the standard QCD analysis [17] while this is not the case for $\pi N \to \mu^+\mu^- X$ [18].

The BB limit seems appropriate for understanding the large single spin asymmetries (SSA) observed in hadron scattering at high x_F and large transverse momenta [6]. The SSA requires quark helicity flip and a dynamical phase, both of which are suppressed in hard subprocesses. The coherence between partons of high and low x allows the helicity flip and phase to occur in the soft part of the amplitude where they are not suppressed.

The multiparton distribution (4.4) that describes the soft dynamics of the Drell-Yan process in the BB limit is a forward target matrix element with four quark fields, which would be of higher twist in the usual Bj limit of fixed x_F. It differs from the MPD's studied by Jaffe [15] in that the two pairs of quark fields originating from the amplitude

– 11 –

and its complex conjugate are evaluated at a finite LF time difference y_3^+. This is a consequence of the finite (in the target rest frame) 'minus' momentum $(1 + x_M)p^-$ of the inclusive system and means that the ordering of the quark fields in the matrix element is significant. For $x_M \to \infty$ we demonstrated that the main contribution to the MPD is from a contraction of a pair of quark fields, which reduces the MPD to a standard leading twist parton distribution.

Acknowledgments

A. The virtual photon and pion wave functions

We use LF polarization vectors [19] for the virtual photon with helicity λ,

$$\varepsilon_\lambda(q) = e_\lambda - \frac{e_\lambda \cdot q}{q^+}n \tag{A.1}$$

with

$$e_{\pm 1} = -\frac{1}{\sqrt{2}}(0, 0, \pm 1, i) \qquad\qquad n = (0, 2, 0, 0) \tag{A.2}$$

$$e_0(q) = -\frac{iq}{\sqrt{q^2}} \qquad\qquad \tilde{n} = (2, 0, 0, 0)$$

which satisfy

$$\sum_{\lambda=\pm 1,0} \varepsilon_\lambda^\mu(k)\,\varepsilon_\lambda^\nu(k)^* = -g^{\mu\nu} + \frac{k^\mu k^\nu}{k^2} \tag{A.3}$$

The pion valence state is defined by its wave function $\Psi_{\boldsymbol{k}}$,

$$|\pi(\boldsymbol{k})\rangle = \sum_{s,A} \frac{(-1)^{s-\frac{1}{2}}}{\sqrt{2N_c}} \int \frac{d^3\boldsymbol{k}_1\,\Psi_{\boldsymbol{k}}(\boldsymbol{k}_1)}{\sqrt{4|\boldsymbol{k}_1||\boldsymbol{k}_2|}(2\pi)^3} b_{s,A}^\dagger(\boldsymbol{k}_1)d_{-s,A}^\dagger(\boldsymbol{k}_2)|0\rangle \tag{A.4}$$

where $\boldsymbol{k}_2 = \boldsymbol{k} - \boldsymbol{k}_1$. The sum is over the helicity $s = \pm\frac{1}{2}$ and color A ($N_c = 3$). With

$$\left\{ b_{s,A}(\boldsymbol{k}_1), b_{s',A'}^\dagger(\boldsymbol{k}_1') \right\} = (2\pi)^3 2|\boldsymbol{k}_1|\delta^3(\boldsymbol{k}_1 - \boldsymbol{k}_1')\delta_{ss'}\delta_{AA'} \tag{A.5}$$

this gives the normalization

$$\langle\pi(\boldsymbol{k}')|\pi(\boldsymbol{k})\rangle = (2\pi)^3 2|\boldsymbol{k}|\delta^3(\boldsymbol{k} - \boldsymbol{k}') \int \frac{d^3\boldsymbol{k}_1}{(2\pi)^3 2|\boldsymbol{k}|}|\Psi_{\boldsymbol{k}}(\boldsymbol{k}_1)|^2 \tag{A.6}$$

Due to the large virtuality of the gluon propagator q_1 in figure 1 only transversally compact valence Fock states contribute at leading order, involving the pion distribution amplitude

$$\phi_\pi(z) \equiv \int \frac{d^2\boldsymbol{k}_{1\perp}}{2(2\pi)^3}\Psi_{\boldsymbol{k}}(\boldsymbol{k}_1) \tag{A.7}$$

where $k_1^- = zk^-$ as in (2.4). With $f_\pi \simeq 93 \, \text{MeV}$ the normalization is

$$\int_0^1 dz \, \phi_\pi(z) = -\frac{f_\pi}{2\sqrt{N_c}} \tag{A.8}$$

Since we took the pion to move along the $-z$ direction in (2.1) we define the LF spinors [19] in the quark operator

$$\psi(y) = \int \frac{d^3\boldsymbol{p}}{2|\boldsymbol{p}|(2\pi)^3} \sum_s \left[b_s(\boldsymbol{p})u_s(\boldsymbol{p})e^{-ip\cdot y} + d_s^\dagger(\boldsymbol{p})v_s(\boldsymbol{p})e^{ip\cdot y} \right] \tag{A.9}$$

to be well-defined for $k^+ = 0$,

$$u(p,s) = \frac{1}{\sqrt{p^-}}\slashed{p}\,\chi(s)$$
$$v(p,s) = \frac{1}{\sqrt{p^-}}\slashed{p}\,\chi(-s) \tag{A.10}$$

where $\chi(\frac{1}{2}) = (1,0,1,0)^T/\sqrt{2}$ and $\chi(-\frac{1}{2}) = (0,1,0,-1)^T/\sqrt{2}$.

At lowest order the Bethe-Salpeter wave function of the pion is

$$\Phi_{\boldsymbol{k}}^{\alpha\beta}(y_1,y_2) \equiv \langle 0|\bar{\psi}_\beta^B(y_2)\psi_\alpha^A(y_1)|\pi(\boldsymbol{k})\rangle \tag{A.11}$$

$$= \frac{\delta_{AB}}{\sqrt{2N_c}}\sum_s(-1)^{s-\frac{1}{2}}\int\frac{d^3\boldsymbol{k}_1\,\Psi_{\boldsymbol{k}}(\boldsymbol{k}_1)}{\sqrt{4|\boldsymbol{k}_1||\boldsymbol{k}_2|}(2\pi)^3}\bar{v}_\beta(\boldsymbol{k}_2,-s)u_\alpha(\boldsymbol{k}_1,s)\exp(-ik_1\cdot y_1 - ik_2\cdot y_2)$$

For the LF spinors defined in (A.10),

$$\sum_s(-1)^{s-\frac{1}{2}}\bar{v}_\beta(\boldsymbol{k}_2,-s)u_\alpha(\boldsymbol{k}_1,s) = \frac{1}{\sqrt{k_1^-k_2^-}}\sum_s(-1)^{s-\frac{1}{2}}(\slashed{k}_1)_{\alpha\alpha'}\chi_{\alpha'}(s)(\gamma^0\chi)_{\beta'}^\dagger(s)(\slashed{k}_2)_{\beta'\beta}$$

$$= \frac{-1}{2\sqrt{k_1^-k_2^-}}[\slashed{k}_1\slashed{n}\gamma_5\slashed{k}_2]_{\alpha\beta} \simeq \frac{1}{2}\sqrt{k_1^-k_2^-}\,[\slashed{n}\gamma_5]_{\alpha\beta} \tag{A.12}$$

where the last equality applies in the limit $k^- \to \infty$, using $\slashed{k}_i \simeq \frac{1}{2}k_i^-\slashed{n}$. Thus

$$\Phi_{k^-\to\infty}^{\alpha\beta}(y_1,y_2) = \frac{\delta_{AB}}{2\sqrt{2N_c}}[\slashed{n}\gamma_5]_{\alpha\beta}\,k^-\int\frac{dz\,d^2\boldsymbol{k}_{\perp 1}}{16\pi^3}\,\Psi_{\boldsymbol{k}}\left(k_1^z = -\frac{1}{2}zk^-,\boldsymbol{k}_{\perp 1}\right)\exp(-ik_1\cdot y_1 - ik_2\cdot y_2) \tag{A.13}$$

With $k_1^+ = k_2^+ = 0$ as in (2.4) the BS wave function $\Phi_{k^-\to\infty}^{\alpha\beta}(y_1,y_2)$ is independent of y_1^-, y_2^-. Thus the wave function is the same whether evaluated at $y_1^- = y_2^-$ (the LF wave function for a particle moving in the $-z$ direction) or at equal ordinary time, $y_1^- - y_2^- = y_2^+ - y_1^+$. This expresses the well-known fact that equal time wave functions are the same as LF wave functions in the infinite momentum frame.

In the BB limit we have $y_{i\perp} = 0$ ($i = 1,2$), hence the pion enters through its distribution amplitude (A.7). In analogy to (3.2) we can write an effective Feynman rule for the pion

$$u_\beta(k_1)\bar{v}_\alpha(k_2) \to \int\frac{dk_1^-}{2\pi}\frac{dy_1^+}{2}\exp\left(\frac{1}{2}ik_1^-y_1^+\right)\langle 0|\bar{\psi}_\beta^B(0)\psi_\alpha^A(y_1)|\pi(\boldsymbol{k})\rangle_{y_1^-=y_{1\perp}=0} \tag{A.14}$$

$$= \int\frac{dk_1^-}{2\pi}\frac{dy_1^+}{2}\Phi_{\boldsymbol{k}}^{\alpha\beta}(y_1^+,0)\exp\left(\frac{1}{2}ik_1^-y_1^+\right)\underset{k^-\to\infty}{\simeq}\frac{\delta_{AB}}{2\sqrt{2N_c}}[\slashed{n}\gamma_5]_{\alpha\beta}\,k^-\int dz\,\phi_\pi(z)$$

which will be multiplied by $k_1^- = zk^-$-dependent propagators, cf. (2.6).

B. The limit of large $x_M p^- = k^-(1 - x_F)$

In the BB limit of the DY process $\pi^+ N \to \gamma^* X$ the virtual photon carries nearly all $(x_F \to 1)$ of the pion momentum, leaving a finite (in the target rest frame) transfer $x_M p^- = k^-(1 - x_F)$ to the target system. In this appendix we consider the case $x_M \gg 1$, when the momentum transfer $(l_1 - l_2)^-$ is large compared to p^-. Since the quark lines l_1, l_2 attach to the non-perturbative GPD their virtualities $l_i^2 = l_i^+ l_i^- - l_{i\perp}^2$ should remain of $\mathcal{O}\left(\Lambda_{\text{QCD}}^2\right)$. Given that $(l_2 - l_1)^+ = x_B p^+$ is fixed either l_1^- or $-l_2^-$, but not both, can grow large. When l_1^- is large the $u(l_1)$-quark hadronizes independently of the target remnants, similarly to the struck quark in the standard Bjorken limit of the DY process. Here we show that the target MPD in the expression (4.7) of the DY cross section reduces to the d-quark PDF as $x_M p^- \simeq l_1^- \to \infty$, and to the $\bar{u}$-quark PDF as $x_M p^- \simeq -l_2^- \to \infty$.

(i) $f_{d\bar{u}/p} \to f_{d/p}$ as $x_M \to \infty$ with $x_M p^- \simeq l_1^-$

According to the expression (4.4) of the MPD the LF time difference between the quark fields $y_3^+ \sim 1/x_M p^- \to 0$ as $x_M \to \infty$. The dynamics then becomes light-cone dominated and contractions of the u- or d-quark fields in the MPD dominate. A contraction turns the MPD into a standard PDF in which the field ordering is irrelevant, i.e. , only one contraction is possible.

The contribution where the u-quark has large momentum and is treated as a free final state particle ($l_1^- \to \infty$, $l_1^+ \sim \Lambda_{\text{QCD}}^2/l_1^-$) corresponds to contracting the u-fields in $f_{d\bar{u}/p}$ of (4.4). Using

$$\langle 0|\psi(x)\bar{\psi}(0)|0\rangle = \int \frac{d^3\boldsymbol{l}}{(2\pi)^3 2|\boldsymbol{l}|} e^{-il \cdot x} \slashed{l} \bigg|_{l^0 = |\boldsymbol{l}|} = \int \frac{dl^+ d^2\boldsymbol{l}_\perp}{(2\pi)^3 2l^+} \theta(l^+) e^{-il \cdot x} \slashed{l} \bigg|_{l^- = l_\perp^2/l^+} \tag{B.1}$$

we have

$$f_{d\bar{u}/p} = \frac{1}{4(4\pi)^3} \int dy_1^- dy_2^- dy_3^- dy_3^+ \exp\left\{\frac{1}{2}i\left[-y_1^- l_1^+ + y_2^- l_1^{+\prime} - y_3^- q^+ + y_3^+ x_M p^-\right]\right\}$$

$$\times \int \frac{dl^+ d^2\boldsymbol{l}_\perp}{(2\pi)^3 2l^+} \theta(l^+) 2l^+ \langle N(p)|\bar{\psi}_d(y_3)\gamma^+ \psi_d(0)|N(p)\rangle$$

$$\times \exp\left[-\frac{1}{2}il^+(y_2^- + y_3^- - y_1^-) - \frac{1}{2}i\frac{l_\perp^2}{l^+}y_3^+\right] \tag{B.2}$$

Integrating over the transverse momenta,

$$\int d^2\boldsymbol{l}_\perp \exp\left[-i\frac{l_\perp^2}{2l^+} y_3^+\right] = -\frac{2\pi i l^+}{y_3^+ - i\varepsilon} \tag{B.3}$$

Given the small effective range of $y_3^+ \sim 1/(k^-(1 - x_F))$ we may neglect the y_3^+-dependence of the matrix element in (B.2) (which is regular on the light-cone). We get

$$\int dy_3^+ \frac{\exp[\frac{1}{2}iy_3^+ k^-(1 - x_F)]}{y_3^+ - i\varepsilon} = 2\pi i \tag{B.4}$$

The integrals over y_1^- and y_2^- give δ-functions constraining $l_1^+ = l_1'^+$ and $l^+ = l_1^+$. Noting that $l_2^+ = q^+ + l_1^+$ we have

$$f_{d\bar{u}/p} = \delta(l_1^+ - l_1'^+)\frac{l_1^+}{4\pi}\theta(l_1^+)f_{d/p}(l_2^+/p^+) \tag{B.5}$$

where the d-quark PDF is

$$f_{d/p}(l_2^+/p^+) = \frac{1}{8\pi}\int dy_3^- \exp\left(-\frac{1}{2}iy_3^- l_2^+\right)\langle N(p)|\bar{\psi}_d(y_3^-)\gamma^+\psi_d(0)|N(p)\rangle \tag{B.6}$$

The dominant contribution to the cross section (4.7) comes from the region of low $l_1^+ = xp^+$ due to $|C(x_B, x)|^2 \propto 1/x^2$ (the other singularity at $x = -x_B$ is outside the kinematic region since $l_1^+ > 0$). This is consistent with $l_1^+ \propto 1/l_1^- \to 0$ at large l_1^-, which ensures that the independently hadronizing u-quark is nearly on-shell. Thus

$$C(x_B, x) \simeq \frac{e_d}{x}\int\frac{dz}{z}\phi_\pi(z) \tag{B.7}$$

Using this and the expression (B.5) for the MPD in the cross section (4.7) we get

$$\frac{d\sigma(\pi^+ N \to \gamma_L^* X)}{dM_X^2} = \frac{(ee_d g^2 C_F)^2}{Q^2 s^2(1-x_B)N_c}\int\frac{dl_1^+}{2\pi l_1^+}\theta(l_1^+)\left(\int\frac{dz}{z}\phi_\pi(z)\right)^2 f_{d/p}(l_2^+/p^+) \tag{B.8}$$

(ii) *Comparison with standard factorization*

We should compare the cross section (B.8) with a calculation [3] where $\sigma(\pi^+ + N \to u + \gamma_L^*(q) + X)$ is expressed in terms of the hard subprocess cross section $\hat{\sigma}(\pi^+(k) + d(l_2) \to u(l_1) + \gamma_L^*(q))$ convoluted with $f_{d/p}(l_2^+/p^+)$. Parametrizing the momenta as

$$\begin{aligned}
l_1 &= (l_1^+, l_1^-, \boldsymbol{l}_\perp)\\
q &= (q^+, q^-, -\boldsymbol{l}_\perp)\\
l_2 &= (l_2^+, 0^-, \boldsymbol{0}_\perp)
\end{aligned} \tag{B.9}$$

we have $l_1^- \simeq x_M p^-$, $l_1^+ = l_2^+ - q^+$, $l_\perp^2 = l_1^+ l_1^-$ and $Q^2 \simeq q^+ q^-$. The subprocess amplitude is in the BB limit

$$\hat{T}(\pi^+ d \to u + \gamma_L^*) = \mp\frac{4iee_d g^2 C_F}{Q\sqrt{2N_c}}\sqrt{\frac{l_2^+}{l_1^+}}\int\frac{dz}{z}\phi_\pi(z) \tag{B.10}$$

where the signs correspond to the helicity $\pm\frac{1}{2}$ of the u-quark. The subprocess cross section

$$\begin{aligned}
\hat{\sigma}(\pi^+ d \to u + \gamma_L^*) &= \frac{1}{16\pi\hat{s}}\int dl_1^+\,\theta(l_1^+)\,dq^-\,dl_\perp^2\,\delta(l_1^+ l_1^- - l_\perp^2)\,\delta(q^+ q^- - Q^2)|\hat{T}|^2\\
&= \frac{(ee_d g^2 C_F)^2}{Q^4 N_c}\int\frac{dl_1^+}{2\pi l_1^+}\theta(l_1^+)\left(\int\frac{dz}{z}\phi_\pi(z)\right)^2 \tag{B.11}
\end{aligned}$$

– 15 –

gives the full cross section

$$\sigma(\pi^+ N \to u + \gamma_L^* + X) = \int \frac{dl_2^+}{p^+} \hat{\sigma}(\pi^+ d \to u + \gamma_L^*) \, f_{d/p}\left(\frac{l_2^+}{p^+}\right) \tag{B.12}$$

Using $dl_2^+ = dq^+ = dM_X^2 \, Q^2/[sk^-(1-x_B)]$ this expression agrees with (B.8) derived from the MPD.

(iii) $f_{d\bar{u}/p} \to f_{\bar{u}/p}$ as $x_M \to \infty$ with $x_M p^- \simeq -l_2^-$

Finally, we consider the contraction of the d-quark fields in the MPD, which corresponds to $\pi^+ N \to \bar{d} + \gamma_L^* + X$. Similarly to (B.1) we have

$$\langle 0|\bar{\psi}_d^\alpha(y_3)\psi_d^\beta(0)|0\rangle = \int \frac{dl^+ \, d^2 \boldsymbol{l}_\perp}{(2\pi)^3 2l^+} \theta(l^+) \, e^{-il \cdot y_3} l^{\beta\alpha}\bigg|_{l^- = l_\perp^2/l^+} \tag{B.13}$$

After the integrals over $d^2\boldsymbol{l}_\perp$ and dy_3^+ and defining $y^- = y_1^- - y_2^- - y_3^-$ we get (with a minus sign from reordering the fermion fields)

$$f_{d\bar{u}/p} = -\frac{1}{4(4\pi)^3} \int dy_1^- \, dy_2^- \, dy^- \int \frac{dl^+}{2\pi} \, l^+ \theta(l^+) \, \langle N(p)|\bar{\psi}_u(y^-)\gamma^+ \psi_u(0)|N(p)\rangle \tag{B.14}$$

$$\times \exp\left[-\frac{i}{4}(y_1^- - y_2^-)(l_1^+ + l_1'^+) - \frac{i}{4}(y_1^- + y_2^-)(l_1^+ - l_1'^+) - \frac{i}{2}(y_1^- - y_2^- - y^-)(q^+ + l^+)\right]$$

The integrals over y_1^-, y_2^- set $l_1^+ = l_1'^+$ and $l^+ = -l_1^+ - q^+ = -l_2^+$, giving

$$f_{d\bar{u}/p} = \delta(l_1^+ - l_1'^+) \frac{-l_2^+}{4\pi} \theta(-l_2^+) f_{\bar{u}/p}(-l_1^+/p^+) \tag{B.15}$$

where the antiquark PDF is

$$f_{\bar{u}/p}(-l_1^+/p^+) = -\frac{1}{8\pi} \int dy^- \exp(-\tfrac{1}{2} iy^- l_1^+)\langle N(p)|\bar{\psi}_u(y^-)\gamma^+ \psi_u(0)|N(p)\rangle \tag{B.16}$$

Now the dominant contribution of $C(x_B, x)$ in the cross section comes from its pole at $l_2^+ = 0$, giving $\sigma \propto e_u^2$ as expected.

References

[1] J. Blümlein and H. Böttcher, *Higher twist contributions to the structure functions $F_2^p(x, Q^2)$ and $F_2^d(x, Q^2)$ at large x and higher orders*, Phys. Lett. **B 662** (2008) 336 [arXiv:0802.0408].

[2] K.J. Anderson et al., *Evidence for longitudinal photon polarization in muon pair production by pions*, Phys. Rev. Lett. **43** (1979) 1219;
J.P. Alexander et al., *Longitudinal photon polarization in muon pair production at high x_F*, Phys. Rev. **D 34** (1986) 315;
J.G. Heinrich et al., *Higher twist effects in the reaction $\pi^- N \to \mu^+\mu^- X$ at $253\,GeV/c$*, Phys. Rev. **D 44** (1991) 1909.

[3] E.L. Berger and S.J. Brodsky, *Quark structure functions of mesons and the Drell-Yan process*, *Phys. Rev. Lett.* **42** (1979) 940;
E.L. Berger, *Higher twist effects in deep inelastic scattering*, *Phys. Lett.* **B 89** (1980) 241;
A. Brandenburg, S.J. Brodsky, V.V. Khoze and D. Mueller, *Angular distributions in the Drell-Yan process: a closer look at higher twist effects*, *Phys. Rev. Lett.* **73** (1994) 939 [hep-ph/9403361];
K.J. Eskola, P. Hoyer, M. Vänttinen and R. Vogt, *Higher twist effects in the Drell-Yan angular distribution*, *Phys. Lett.* **B 333** (1994) 526 [hep-ph/9404322].

[4] C. Biino et al., *J/ψ longitudinal polarization from πN interactions*, *Phys. Rev. Lett.* **58** (1987) 2523.

[5] S.J. Brodsky, P. Hoyer, A.H. Mueller and W.-K. Tang, *New QCD production mechanisms for hard processes at large x*, *Nucl. Phys.* **B 369** (1992) 519.

[6] P. Hoyer and M. Järvinen, *Single spin asymmetry at large x_F and $k_\perp$*, *JHEP* **02** (2007) 039 [hep-ph/0611293].

[7] J.D. Bjorken, *Deep-inelastic electroproduction*, in *Proceedings of the conference on particle physics*, *Irvine California U.S.A.* 1971, M. Bander, G. Shaw and D. Wong eds., *AIP Conf. Proc.* **6** (1972) 151, AIP, New York U.S.A.;
J.D. Bjorken and J. Kogut, *Correspondence arguments for high-energy collisions*, *Phys. Rev.* **D 8** (1973) 1341;
J.D. Bjorken, *Rapidity gaps in deep inelastic scattering*, talk at conference on *Fundamental Interactions of Elementary Particles*, ITEP, Moscow Russia (1995), SLAC-PUB-7096 (1996), [hep-ph/9601363];
P. Hoyer, *The unexpected role of final state interactions in deep inelastic scattering*, in *Proceedings of the Conference on I. Ya. Pomeranchuk and Physics at the Turn of the Centuries, Moscow Russia*, World Scientific, Singapore (2004) [hep-ph/0307263].

[8] S.J. Brodsky, P. Hoyer, N. Marchal, S. Peigne and F. Sannino, *Structure functions are not parton probabilities*, *Phys. Rev.* **D 65** (2002) 114025 [hep-ph/0104291].

[9] A.V. Efremov and A.V. Radyushkin, *Factorization and asymptotical behavior of pion form-factor in QCD*, *Phys. Lett.* **B 94** (1980) 245;
G.P. Lepage and S.J. Brodsky, *Exclusive processes in quantum chromodynamics: evolution equations for hadronic wave functions and the form-factors of mesons*, *Phys. Lett.* **B 87** (1979) 359.

[10] E.R. Berger, M. Diehl and B. Pire, *Probing generalized parton distributions in $\pi N \to \ell^+\ell^- N$*, *Phys. Lett.* **B 523** (2001) 265 [hep-ph/0110080].

[11] M. Diehl, *Generalized parton distributions*, *Phys. Rept.* **388** (2003) 41 [hep-ph/0307382].

[12] J.C. Collins, L. Frankfurt and M. Strikman, *Factorization for hard exclusive electroproduction of mesons in QCD*, *Phys. Rev.* **D 56** (1997) 2982 [hep-ph/9611433].

[13] L.L. Frankfurt, P.V. Pobylitsa, M.V. Polyakov and M. Strikman, *Hard exclusive pseudoscalar meson electroproduction and spin structure of a nucleon*, *Phys. Rev.* **D 60** (1999) 014010 [hep-ph/9901429];
T. Feldmann and P. Kroll, *Skewed parton distributions for $B \to \pi$ transitions*, *Eur. Phys. J.* **C 12** (2000) 99 [hep-ph/9905343];
B. Pire and L. Szymanowski, *Hadron annihilation into two photons and backward VCS in the scaling regime of QCD*, *Phys. Rev.* **D 71** (2005) 111501 [hep-ph/0411387]; *A QCD analysis*

of $\bar{p}N \to \gamma^*\pi$ and $\bar{p}N \to \gamma^*\gamma$. Where is the pion in the proton?, PoS(HEP2005)103 [hep-ph/0509368].

[14] B. Pire and L. Szymanowski, *QCD analysis of $\bar{p}N \to \gamma^*\pi$ in the scaling limit, Phys. Lett.* **B 622** (2005) 83 [hep-ph/0504255].

[15] R.L. Jaffe, *Parton distribution functions for twist four, Nucl. Phys.* **B 229** (1983) 205.

[16] W. Melnitchouk, R. Ent and C. Keppel, *Quark-hadron duality in electron scattering, Phys. Rept.* **406** (2005) 127 [hep-ph/0501217];
Quark models of duality in electron and neutrino scattering, proceedings of the 1$^{\rm st}$ *Workshop on Quark-Hadron Duality and the Transition to pQCD, Frascati Italy June 6–8 2005,* http://www.lnf.infn.it/conference/duality05/, World Scientific, Singapore (2006) [ISBN:981-256-684-8].

[17] FNAL-E866/NuSea collaboration, L.Y. Zhu et al., *Measurement of angular distributions of Drell-Yan dimuons in $p + d$ interaction at $800\,GeV/c$, Phys. Rev. Lett.* **99** (2007) 082301 [hep-ex/0609005].

[18] NA10 collaboration, S. Falciano et al., *Angular distributions of muon pairs produced by $194\,GeV/c$ negative pions, Z. Physik* **C 31** (1986) 513;
NA10 collaboration, M. Guanziroli et al., *Angular distributions of muon pairs produced by negative pions on deuterium and tungsten, Z. Physik* **C 37** (1988) 545;
J.S. Conway et al., *Experimental study of muon pairs produced by $252\,GeV$ pions on tungsten, Phys. Rev.* **D 39** (1989) 92;
J.G. Heinrich et al., *Higher twist effects in the reaction $\pi^- N \to \mu^+\mu^- X$ at $253\,GeV/c$, Phys. Rev.* **D 44** (1991) 1909.

[19] S.J. Brodsky, H.-C. Pauli and S.S. Pinsky, *Quantum chromodynamics and other field theories on the light cone, Phys. Rept.* **301** (1998) 299 [hep-ph/9705477].